A Further Contribution to the Parametric Analysis of a PCM Energy Storage System

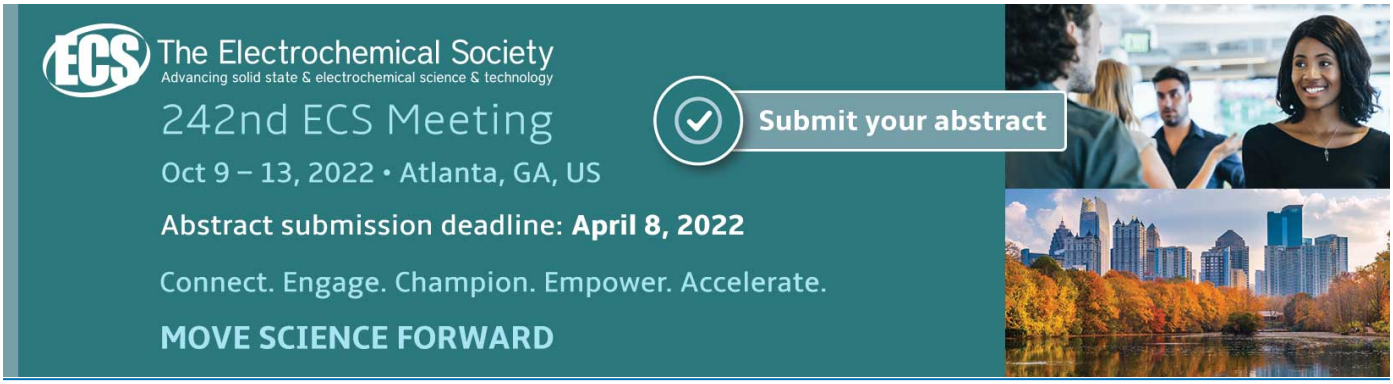

IOP Conf. Series: Journal of Physics: Conf. Series **796** (2017) 012029 doi:10.1088/1742-6596/796/1/012029

A Further Contribution to the Parametric Analysis of a PCM Energy Storage System

G Casano and S Piva

ENDIF ENgineering Department In Ferrara, Università di Ferrara
via Saragat 1, 44122 Ferrara (I)

Corresponding Author E-mail: stefano.piva@unife.it

Abstract. In recent years heat storage using phase change materials has been also considered in the thermal control of electronic devices. In a recent work we presented some results for a parametric analysis of an energy storage system with a phase change material undergoing a two-levels steady-periodic heat boundary condition, as happens in certain electronic equipments. In particular, a hybrid system composed of a finned surface partially filled with a PCM, was analysed. This solution, which combines both passive (PCM) and active (fins and fans) cooling solutions, is of interest in high power amplifiers characterized by different levels of power dissipation, as is the case of the telecom base station power amplifiers, where the power is proportional to the traffic load. In the present paper we analyze some parameter previously not investigated, in particular the dimensionless transition temperature, for the role played by this parameter in the limitation of the operating temperature reached during the peaks of the power input. The study has provided further useful information for the design of these hybrid cooling systems..

1. Introduction

Heat storage systems using Phase Change Materials (PCMs in the following) offer effective opportunities for managing thermal energy due to the high energy storage density and the isothermal nature of the storage process. Beside interesting applications in many different fields (building envelopes, residential heating and cooling, solar engineering, and spacecraft thermal control applications [1]), in recent years latent heat storage has been also considered in the thermal control of electronic devices, where the heat generated by electronic circuitry must be dissipated to prevent immediate failure and assure long term reliability. In particular for high specific power and/or compactness, the limited capability of the air cooling traditional techniques suggests to benefit from the advantages offered by PCMs, such as: high specific heat, high latent heat, small volume change during phase change, availability at convenient values of melting temperature, non-toxicity, inertness and non-corrosiveness. Furthermore, PCM energy storage systems can be useful to delay the heat release so to reduce the need of heat transfer surface, in particular when the heat dissipation is of periodic nature or suddenly changing.

For a large review of the applications of latent heat storage in electronics some recent papers and volumes are available (Srivatsan *et al.* [2], Ling *et al.* [3], Fleischer [4], Castell and Solé. [5], Casano and Piva [6]).

In some recent papers ([6] and [7]) we presented some results for applications dealing with high power amplifiers characterized by different levels of power dissipation, as is the case of the telecom base station power amplifiers, where the power is proportional to the traffic load. The final goal of this research is the development of a hybrid PCM heat sink for power electronics applications, consisting of a heat sink with part of the channel between the fins filled of a suitable solid-solid PCM. In [7] we analysed experimentally and numerically a TCU consisting of a plane slab of PCM for an on/off heating condition. In [6] we presented some results of a parametric analysis, based on a numerical investigation, for a finned heat sink partially filled of solid-solid PCM. The mathematical model was made dimensionless to allow the characteristic parameters of the application to be evidenced and discussed. However, the large number of independent dimensionless parameters (13) suggested in [6] to concentrate our attention on a limited number of parameters (4), two useful to describe the thermal load and two to characterize the thermal behaviour of the TCU.

In the present paper we add some new results, useful to extend the analysis to some parameter previously not investigated. In particular we concentrate now our attention to the dimensionless transition temperature for the role played by this parameter in the limitation of the operating temperature reached during the peak of the input power. Some new useful information can be now suggested for the design of these hybrid cooling systems.

2. Mathematical Formulation

A sketch of the physical system, consisting of a finned heat transfer surface partially filled of PCM, is shown in figure 1. The heat sink is heated by the electronic system and cooled by a forced flow of air. For the large number of fins and the boundary conditions, when neglecting the longitudinal dependency in the temperature distribution, the analysis can be limited to a 2D portion of the system (figure 2).

The mathematical model representing the physical process is based on the following assumptions:

- PCM is homogeneous and isotropic.
- Thermophysical properties are constant in each phase.
- Phase-change occurs at a single transition temperature between the two solid phases.
- Heat transfer is controlled only by conduction.
- The problem is two-dimensional.

The problem is governed by the Fourier equation, to be solved in the two solid phases of the PCM and in the fin ($i = F$ in the fin; $i = S1$ or $S2$ for the two solid phases of the PCM; $S1$ indicates the area where $T < T_f$, $S2$ that where $T > T_f$).

As the boundary conditions, on the basement a uniform, a time-dependent heat load is applied, characterised by two levels of power. The duty cycle (figure 3) is periodic, with a low power period (q_1 for $0 \le t \le t_1$) and a high power period (q_2 for $t_1 < t < P$). The portion of the fin free in air, for

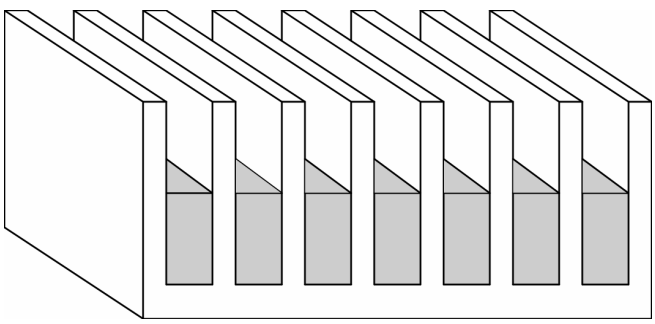

Figure 1. Scheme of the finned heat transfer surface.

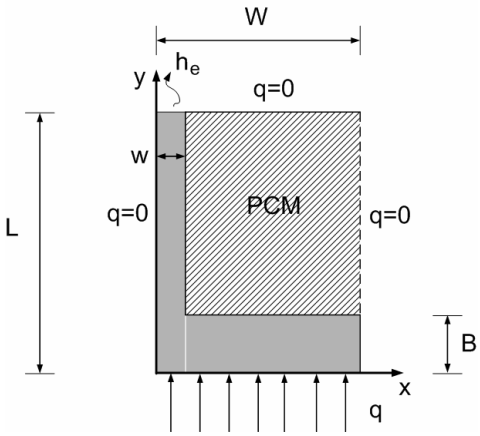

Figure 2. Schematic diagram of the reference domain of the finned heat transfer surface.

simplicity reasons, is substituted by an equivalent heat transfer coefficient, *he**, sized to accommodate the high level heat load. It allows the system to operate during the low power portion of the duty cycle at a value of temperature that is certainly below the transition temperature of the PCM. The remaining surfaces are adiabatic.

The full set of differential equations and boundary conditions is reported in [6]. For reason of brevity here only their dimensionless form is shown. The problem can be thence stated in mathematical form as follows (see the Nomenclature for the definition of the dimensionless quantities):

• Solid phases (for fin, solid 1 and solid 2, respectively):

$$\frac{\partial \theta}{\partial \tau} = Fo_F \mathrm{A}_i \left(\frac{\partial^2 \theta}{\partial \xi^2} + \frac{\partial^2 \theta}{\partial \eta^2} \right) \tag{1}$$

• Solid–solid interface:

$$\theta_{S1} = \theta_{S2} = \theta_f \tag{2}$$

$$\frac{1}{\mathrm{A}_{S1} Fo_F Ste} \frac{\partial \Xi}{\partial \tau} = \left[1 + \left(\frac{\partial \Xi}{\partial \xi} \right)^2 \right] \left(\frac{\partial \theta_{S1}}{\partial \eta} - \frac{\Lambda_{S2}}{\Lambda_{S1}} \frac{\partial \theta_{S2}}{\partial \eta} \right) \tag{3}$$

• Initial condition:

$$\tau = 0 \ , \ 0 \le \xi \le 1 \quad \text{and} \quad 0 \le \eta \le 1 \quad \theta(\xi, \eta, \tau = 0) = 0 \tag{4}$$

• Boundary conditions:

$$\xi = 0 \quad \text{and} \quad 0 \le \eta \le 1 \quad \frac{\partial \theta}{\partial \xi} = 0 \ \text{ for } \quad 0 < \tau \le 1 \tag{5}$$

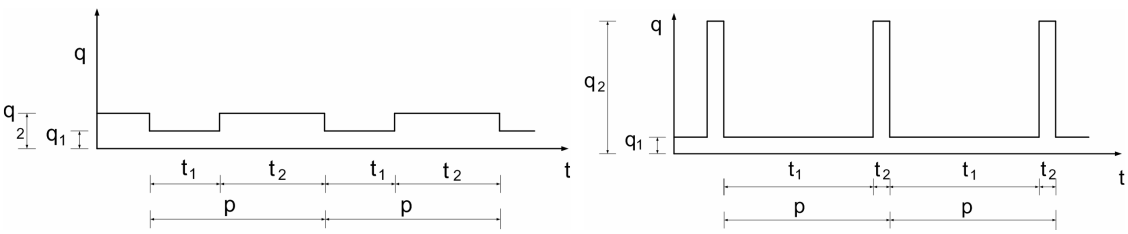

Figure 3. Typical duty cycle of the heating system.

$$\xi = \xi_W \quad \text{and} \quad 0 \le \eta \le 1 \quad \frac{\partial \theta}{\partial \xi} = 0 \quad \text{for} \quad 0 < \tau \le 1 \tag{6}$$

$$\eta = 0 \quad \text{and} \quad 0 \le \xi \le \xi_W \quad \frac{\partial \theta_F}{\partial \xi} = -1 \quad \text{for} \quad 0 < \tau \le \tau_1 \tag{7}$$

$$\eta = 0 \quad \text{and} \quad 0 \le \xi \le \xi_W \quad \frac{\partial \theta_F}{\partial \xi} = -\Omega \quad \text{for} \quad \tau_1 < \tau \le 1 \tag{8}$$

$$\eta = 1 \quad \text{and} \quad 0 \le \xi \le \xi_w \quad \frac{\partial \theta_F}{\partial \eta} = \frac{Bi}{\xi_W}\left(\theta_F - \theta_{ai}\right) \quad \text{for} \quad 0 < \tau \le 1 \tag{9}$$

$$\eta = 1 \quad \text{and} \quad \xi_w < \xi \le \xi_W \quad \frac{\partial \theta}{\partial \eta} = 0 \quad \text{for} \quad 0 < \tau \le 1 \tag{10}$$

$$\xi = \xi_w \quad \text{and} \quad \eta_B \le \eta \le 1 \quad \frac{\partial \theta_F}{\partial \xi} = \Lambda_i \frac{\partial \theta_i}{\partial \xi} \quad \text{for} \quad 0 < \tau \le 1 \tag{11}$$

$$\eta = \eta_B \quad \text{and} \quad \xi_w < \xi \le \xi_W \quad \frac{\partial \theta_F}{\partial \eta} = \Lambda_i \frac{\partial \theta_i}{\partial \eta} \quad \text{for} \quad 0 < \tau \le 1 \tag{12}$$

The significant dimensionless parameters of the problem are:

$$Fo_F,\ Ste,\ Bi,\ \theta_f,\ A_{S1},\ A_{S2},\ \Lambda_{S1},\ \Lambda_{S2},\ \tau_1,\ \Omega,\ \xi_W,\ \xi_w,\ \eta_B.$$

Even though in the mathematical model the dimensionless parameter characterizing the thermal load is τ_1, in the following discussion of the results, we use τ_2 , its complement to 1 ($\tau_2 = 1 - \tau_1$), being this parameter closer to the significance of the heating scheme.

The initial condition, Eq. (4), characterizes an isothermal system at the room temperature. At this time the total energy (sensible and latent) of the system, H_0, is conventionally set $H_0 = 0$.

The time evolution of total energy stored by the system is given by the integral in time of the difference between the incoming and outgoing heat fluxes:

$$\Delta H(t) = \int_0^t \left[q(t) W - \int_0^w h_e \left(T_F(x, L, t) - T_a \right) dx \right] dt \tag{13}$$

where, for the n-th cycle of heating: $q(t) = \begin{cases} q_1 & \text{for} \quad (n-1)P < t \le t_1 + (n-1)P \\ q_2 & \text{for} \quad t_1 + (n-1)P < t \le nP \end{cases}$

The latent energy storage, $\Delta H_L(t)$, is calculated as:

$$\Delta H_L(t) = \rho_{S1} r S_2(t) \tag{14}$$

The sensible energy is calculated as the difference between total and latent energy at the same time.

The reference energy used to make dimensionless the stored energy is the maximum latent energy storable in the system, given by:

$$\left(\Delta H_L\right)_{\max} = \rho_{S1} r S_{PCM} \tag{15}$$

where S_{PCM} indicates the surface filled by the PCM ($S_{PCM} = S_1 + S_2$).

The dimensionless latent and total energy are given, respectively, by:

$$\Delta E_L(\tau) = \frac{\Delta H_L(t)}{\left(\Delta H_L\right)_{\max}} \tag{16}$$

$$\Delta \mathrm{E}(\tau) = \frac{\Delta H_L(t) + \Delta H_S(t)}{(\Delta H_L)_{\max}} \tag{17}$$

For the latent and total energy the amplitude of the difference between the maximum and minimum value reached in a period of heating is given, respectively, by:

$$\Delta \mathrm{E}_L = (\Delta \mathrm{E}_L)_{\max} - (\Delta \mathrm{E}_L)_{\min} \tag{18}$$

$$\Delta \mathrm{E} = (\Delta \mathrm{E})_{\max} - (\Delta \mathrm{E})_{\min} \tag{19}$$

A parameter significant in the thermal design of electronics equipment is the mean temperature, and the corresponding dimensionless mean temperature, on the surface receiving the heat flux, given by, respectively:

$$T_m(t) = \frac{1}{W}\int_0^W T(x,0,t)\,dx \tag{20}$$

$$\theta_m(\tau) = \frac{T_m(t) - T_0}{q_1 L/\lambda_F} \tag{21}$$

The mean temperature is analyzed also in terms of its average value over a period:

$$(T_m)_{av} = \frac{1}{P}\int_{(n-1)P}^{nP} T_m(t)\,dt \tag{22}$$

$$(\theta_m)_{av} = \frac{(T_m)_{av} - T_0}{q_1 L/\lambda_F} \tag{23}$$

For the numerical solution of the problem the Finite Volume Method is used. The numerical procedure and some validation exercises are described in full details in [8]. Here it is relevant to underline that a simplified 2-D approach is followed. Inside each control volume affected by the change of phase, the interface is assumed to advance only in the x direction. The resulting solid/solid transition front assumes thence a stepwise shape. The calculation domain consists of 450 control volumes and the time step is 1 s. The calculations are carried out until the reaching of a steady periodic state.

3. Results and Discussion

In the following discussion, reference will be constantly made to the numerical results produced by Casano and Piva [6] for the same configuration analysed in the present paper.

The problem is highly nonlinear and characterized by a large number of dimensionless parameters. In [6] the discussion was limited to four dimensionless parameters: the Biot number, *Bi*, the power ratio, Ω, the Stefan number, *Ste*, and the time ratio, τ_2. Here we explore the effect of a further dimensionless parameter, the dimensionless temperature of transition, θ_f. For the whole set of simulations we maintained the same dimensionless parameters used in [6]: $\Lambda_{S1} = \Lambda_{S2} = 7.411 \cdot 10^{-4}$, $A_{S1} = 1.122 \cdot 10^{-3}$, $A_{S2} = 1.005 \cdot 10^{-3}$, $\xi_W = 4.082 \cdot 10^{-2}$, $\xi_w = 1.020 \cdot 10^{2}$, $Fo_F = 160.2$, $\eta_B = 2.041 \cdot 10^{-2}$. Furthermore, for simplicity we maintained also the following parameters: $T_0 = 30$ °C, $q_1 = 3000$ W/m^2 and $P = 4500$ s.

In figure 4 some results are shown for a fixed *Ste* (*Ste* = 0.012) and a fixed Ω (Ω = 4), for three values of dimensionless transition temperature (θ_f = 9.64, 16.52, 23.41), and for three Biot numbers (*Bi* = 0.059, 0.078, 0.156). The values of the dimensionless amplitude of total, ΔE, and latent, ΔE_L, energy are shown as a function of the dimensionless time ratio, τ_2. The solid line is used for the dimensionless amplitude of the total energy, ΔE, the dashed line for the dimensionless amplitude of the latent energy, ΔE_L.

The dimensionless amplitude of total and latent energy is zero for $\tau_2 = 0$ (steady heating with a low

power) and for $\tau_2 = 1$ (steady heating with a high power). Both distributions show a maximum in the interval $0 < \tau_2 < 1$. In general, in Figure 4 it is observed that the maximum values of ΔE_L and ΔE, tend to increase with θ_f for the lowest values of *Bi*, and to decrease for the highest value of *Bi*. For the lowest values of *Bi* (*Bi* = 0.059) the maximum of ΔE tends to a value independent of θ_f; the maximum of ΔE occurs for higher values of τ_2 when increasing θ_f. On the opposite, for the highest values of *Bi* (*Bi* = 0.156) the maximum of ΔE changes a lot with θ_f, while it changes a little with τ_2. Between these two values, for *Bi* = 0.078, the maximum of ΔE changes very little with θ_f, while it changes a lot with τ_2. For the lowest values of *Bi* (*Bi* = 0.059) the maximum of ΔE_L increases with θ_f, with a tendency to become less sensible to the variations of τ_2 for the highest values of θ_f. On the opposite, for the highest values of *Bi* (*Bi* = 0.156) the maximum of ΔE_L decreases with θ_f, whit a progressively lower dependency on τ_2. Between these two values, for *Bi* = 0.078, the maximum of ΔE_L changes moderately with θ_f. In order to obtain large movements of the solid-solid interface, large values of θ_f are needed for limited *Bi*, the opposite for large *Bi*.

For the same values of *Ste* and Ω of figure 4, in figure 5 are shown with a solid and a dashed line, the maximum, $(\theta_m)_{max}$ and the average, $(\theta_m)_{av}$, of the dimensionless mean temperature on the heated surface, respectively, as a function of the dimensionless time τ_2. In general in figure 5 it is observed the same trend already discussed in [6]. The distributions of $(\theta_m)_{max}$ are characterized by decreasing values for increasing values of *Bi*, because a better heat transfer due to larger surfaces of the fins in air or a more intensive convection (high *Bi*), coupled to the same energy input (same Ω), is the reason of a decrease of the temperature. For the whole set of data shown in figure 5, for increasing values of τ_2 a value of $(\theta_m)_{max}$ independent of the value of τ_2 is rapidly reached; this is the value of $(\theta_m)_{max}$ due to the highest power, reached for $\tau_2 = 1$. Only for low values of τ_2 a dependency of $(\theta_m)_{max}$ on this parameter is evident. The distributions of the $(\theta_m)_{max}$ are quite independent of θ_f. Only for low values of τ_2 ($\tau_2 <$ 0.2÷0.4) it is possible to observe that for the lowest values of *Bi* the asymptotic region of $(\theta_m)_{max}$ shrinks for increasing values of θ_f , the opposite for the highest values of *Bi*. As already recognized in [6], the distributions of $(\theta_m)_{av}$, for increasing values of τ_2, are characterized by a linear increase between the values corresponding to the low and high power steady heating ($\tau_2 = 0$ and $\tau_2 = 1$). This average temperature is clearly related to the dimensionless input energy into the system, as already shown in [6].

In figure 6 some results are shown of the amplitude of total, ΔE, latent ΔE_L, and sensible, $\Delta E - \Delta E_L$, dimensionless energy as a function of the Stefan number, *Ste*, for three values of dimensionless phase transition temperature ($\theta_f = 9.64, 16.52, 23.41$), and for three Biot numbers (*Bi* = 0.059, 0.078, 0.156), for $\tau_2 = 0.6$ and $\Omega = 4$. The solid line is used for the dimensionless amplitude of the total energy, ΔE, the dashed line for the dimensionless amplitude of the latent energy, ΔE_L. For the same values of *Bi* and θ_f of figure 6, in figure 7 is shown with a solid line and a dashed line the maximum, $(\theta_m)_{\max}$ and the average, $(\theta_m)_{av}$, dimensionless mean temperature on the heated surface, as a function of the Stefan number, *Ste*.

In figure 6, for the whole set of calculations, ΔE increases with *Ste* and ΔE_L tends to an asymptotic value independent of *Ste*. The attainment of this asymptotic value depends on *Bi*, *Ste* and θ_f. In figure 6, the effects of θ_f is evident: for increasing values of θ_f, the limiting value $\Delta E_L = 1$ is attained for decreasing values of *Bi*. For the highest values of *Bi* the asymptotic values of ΔE_L is lower than 1 and decreases with θ_f. The dimensionless amplitude of sensible energy (ΔE-ΔE_L) is independent of θ_f; this explains the different slope of the distributions of ΔE: when the latent storage system attains the maximum oscillation, only the sensible energy contributes to the increase of ΔE.

For the same values of τ_2 and Ω of figure 6, in figure 7 are shown with a solid and a dashed line, the maximum, $(\theta_m)_{max}$ and the average, $(\theta_m)_{av}$, of the dimensionless mean temperature on the heated surface, respectively, as a function of the Stefan number *Ste*. In general in figure 7 is observed the same dependency of *Ste* already discussed in [6]. Small reductions of $(\theta_m)_{max}$ are evident for low values of *Ste*; this effect increases with θ_f. In the whole set of data shown in figure 7, $(\theta_m)_{av}$ is the same for the same *Bi*, because this parameter depends only on the dimensionless input energy, here constant ($\Omega = 4$).

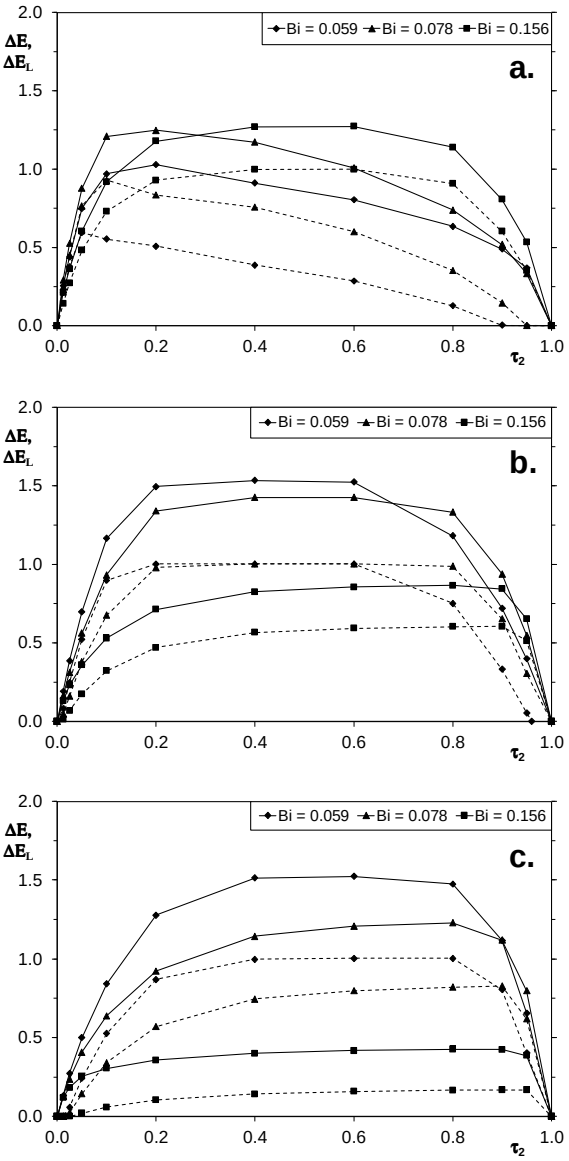

Figure 4. Amplitude of total, ΔE (——), and latent, ΔE_L (– – –), dimensionless energy, for *Ste* = 0.012 and Ω = 4, as a function of τ_2; a.: θ_f = 9.64; b.: θ_f = 16.52; c.: θ_f = 23.41.

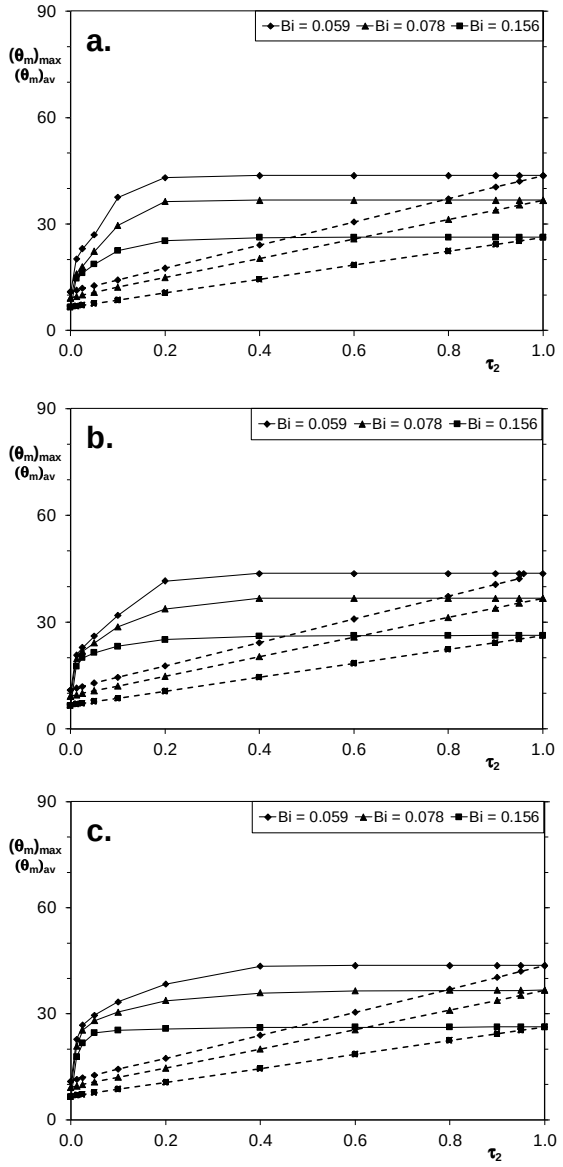

Figure 5. Maximum, $(\theta_m)_{max}$ (——), and average, $(\theta_m)_{av}$ (– – –), dimensionless mean temperature on the heated surface, for *Ste* = 0.012 and Ω = 4, as a function of τ_2; a.: θ_f = 9.64; b.: θ_f = 16.52; c.: θ_f = 23.41.

4. Concluding remarks

A Thermal Control Unit with a PCM energy storage system, designed for the thermal control of electronic devices, has been investigated numerically. This application is characterized by a periodic heating on two levels of power; conduction heat transfer is the prevailing heat transfer process. The main design parameter is the maximum value of average temperature on the heated surface, where the electronic components to be cooled are placed.

The analysis of its energy behaviour shows that the storage of energy varies periodically in time with the two levels of heating.

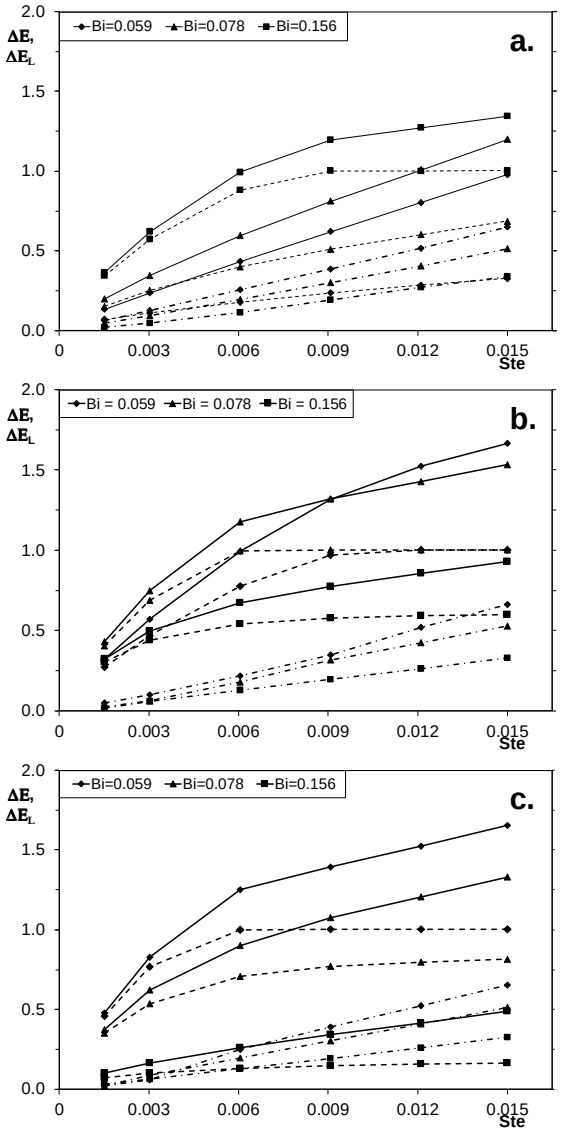

Figure 6. Amplitude of total, ΔE (——), latent, ΔE_L (– – –), and sensible, ΔE-ΔE_L (– · – · –), dimensionless energy, for $\tau_2 = 0.6$ and $\Omega = 4$, as a function of *Ste*; a.: $\theta_f = 9.64$; b.: $\theta_f = 16.52$; c.: $\theta_f = 23.41$.

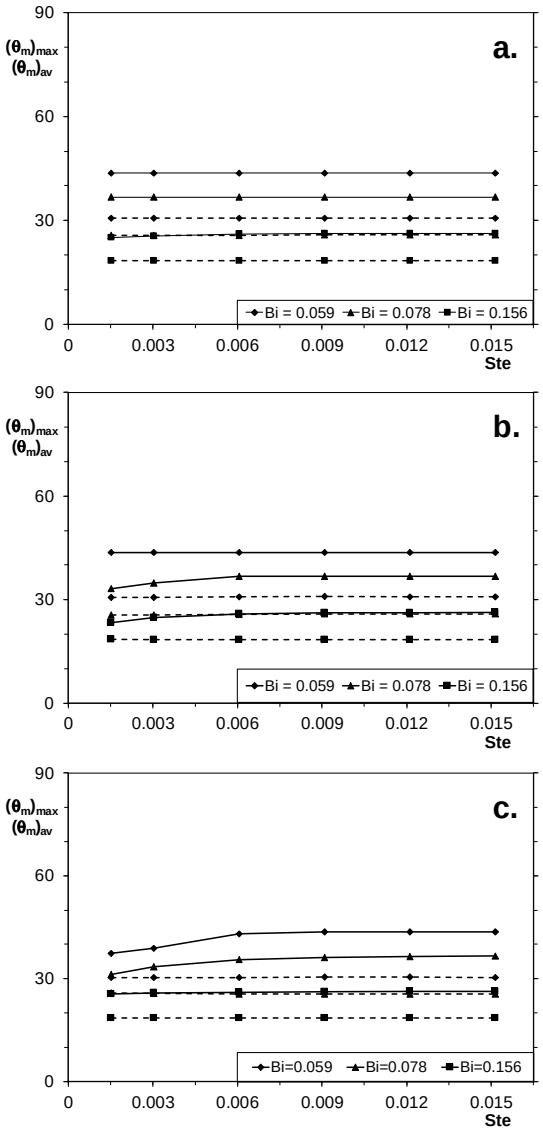

Figure 7. Maximum, $(\theta_m)_{max}$ (——), and average, $(\theta_m)_{av}$ (– – –), dimensionless mean temperature on the heated surface, for $\tau_2 = 0.6$ and $\Omega = 4$, as a function of *Ste*; a.: $\theta_f = 9.64$; b.: $\theta_f = 16.52$; c.: $\theta_f = 23.41$.

In general it can be observed that a Thermal Control Unit using PCM is suitable to be used when a high power heating acts in short times. During the peak of heating, the phase change can occur; afterwards, it is important that the storage system could release the stored energy in a freezing process. For this hybrid heat storage system, in order to exploit the presence of the PCM, it is important to store and to release an amount of latent energy lower than the maximum latent energy storable.

The dimensionless parameters governing the steady periodic process are thirteen; in a previuos paper [6] we concentrated our attention on two parameters useful to describe the thermal load (Ω and τ_2) and on two more parameters useful to characterize the thermal behaviour of the TCU (*Bi* and *Ste*). In the present paper we explore the effects of the dimensionless temperature of transition, θ_f.

When θ_f is low, a high value of *Bi* helps to control the maximum temperature; the contribution of

the PCM to the energy storage can be significant, because a high dissipation to the ambient can sustain the oscillation of the interface position. On the opposite, when θ_f is high, is a low value of *Bi* that helps the complete exploitation of the PCM in terms of oscillations of energy storage. Anyway, in terms of maximum temperature on the heated surface, the behaviour of the Thermal Control Unit seems to be quite independent of θ_f.

A complete exploitation of the PCM requires therefore an accurate design of the system on the base of the parameters affecting the performance of the TCU.

5. References

[1] Sharma A, Tyagi V V, Chen C R and Buddhi D 2009 Review on thermal energy storage with phase change materials and applications *Renewable and Sustainable Energy Reviews* **13** 318-345

[2] Srivatsan S, Anand, J B, Deepak S and Senthil Kumar D 2014 Experimental Analysis of Heat Sinks incorporating Phase Change Materials and Thermal Conductivity Enhancers *Int. J. Engineering Research & Technology (IJERT)* **3** 1197-1204

[3] Ling Z, Zhang Z, Shi G, Fang X, Wang L, Gao X, Fang Y, Xua T, Wang S and Liu X 2014 Review on thermal management systems using phase change materials for electronic components, Li-ion batteries and photovoltaic modules *Renewable and Sustainable Energy Reviews* **31** 427–438

[4] Fleischer A S 2015 *Thermal Energy Storage Using Phase Change Materials. Fundamentals and Applications* (Springer) pp. 8-12

[5] Castell A and Solé C 2015 Design of latent heat storage systems using phase change materials (PCMs) *Advances in Thermal Energy Storage Systems: Methods and Applications* ed. Luisa F. Cabeza (Woodhead Publishing) pp. 298-302

[6] Casano G and Piva S 2015 Parametric Analysis of a PCM Energy Storage System. *Int. J. Heat Technology* **33** 61-68

[7] Casano G and Piva S 2014 Experimental and numerical investigation of a phase change energy storage system *Journal of Physics Conference Series* **501** 012012

[8] Pinelli M, Casano G and Piva S 2000 Solid-liquid phase change heat transfer in a vertical cylinder heated from above *Int. J. Heat and Technology* **18** 61-67

6. Nomenclature

Symbols

B	m	Thickness of the basement
Bi	-	Biot number $(h_e*W)/\lambda_F$
c	J/(kg K)	Specific heat at constant pressure
Fo	-	Fourier number $\alpha_F P/L^2$
h_e*	W/m^{2}K	Equivalent heat transfer coefficient
H	J	Enthalpy
L	m	Height of the fin
P	s	Period
q	W/m^2	Heating power
r	J/kg	Latent heat of transition
Ste	-	Stefan number $c_{S1}T_R/r$
t	s	Time
T	K	Temperature
T_R	K	Reference temperature $q_1 L/\lambda_F$
w	m	Thickness of the fin
W	m	Half width of the fin-PCM system
x	m	Cartesian coordinate
X	m	Solid-solid interface position

y	m	Cartesian coordinate

Greek symbols

α	m^2/s	Thermal diffusivity
A_{Si}	-	Thermal diffusivity ratio α_{Si}/α_F
E	-	Dimensionless energy $\Delta H/(\Delta H_L)_{max}$
η	-	Dimensionless coordinate y/L
θ	-	Dimensionless temperature $(T-T_0)/T_R$
λ	W/(m·K)	Thermal conductivity
Λ_{Si}	-	Thermal conductivity ratio λ_{Si}/λ_F
ξ	-	Dimensionless coordinate x/L
Ξ	-	Dimensionless position of the interface X/L
ρ	kg/m^3	Density
Π	-	Dimensionless input of energy $qt/(\Delta H_L)_{max}$
τ	-	Dimensionless time t/P
τ_i	-	Time ratio t_i/P
Ω	-	Power ratio q_2/q_1

Subscripts

a	Ambient
av	Average over a period
B	Basement
f	Phase change
F	Fin
m	Mean on the heated surface
max	Maximum
min	Minimum
L	Latent
PCM	Phase change material
S1, S2	Different phases of the solid PCM
w	Half thickness of the fin
W	Half width of the fin-PCM system
0	Initial condition
1, 2	Low and high power